Title

An Integrated Framework for Infectious Disease Control Using Mathematical Modeling and Deep Learning.

Authors

Salman, Mohammed
Das, Pradeep
Mohanty, Sanjay

Publication Date

2025

DOI

10.1109/OJEMB.2024.3455801

Peer reviewed

An Integrated Framework for Infectious Disease Control Using Mathematical Modeling and Deep Learning

Mohammed Salman, Pradeep Kumar Das, *Member, IEEE*, and Sanjay Kumar Mohanty

***Abstract*—Infectious diseases are a major global public health concern. Precise modeling and prediction methods are essential to develop effective strategies for disease control. However, data imbalance and the presence of noise and intensity inhomogeneity make disease detection more challenging. *Goal:* In this article, a novel infectious disease pattern prediction system is proposed by integrating deterministic and stochastic model benefits with the benefits of the deep learning model. *Results:* The combined benefits yield improvement in the performance of solution prediction. Moreover, the objective is also to investigate the influence of time delay on infection rates and rates associated with vaccination. *Conclusions:* In this proposed framework, at first, the global stability at disease free equilibrium is effectively analysed using Routh-Haurwitz criteria and Lyapunov method, and the endemic equilibrium is analysed using non-linear Volterra integral equations in the infectious disease model. Unlike the existing model, emphasis is given to suggesting a model that is capable of investigating stability while considering the effect of vaccination and migration rate. Next, the influence of vaccination on the rate of infection is effectively predicted using an efficient deep learning model by employing the long-term dependencies in sequential data. Thus making the prediction more accurate.**

***Index Terms*—Migration, vaccination, stochastic perturbation, Lyapunov stability, volterra integral equation, long short term memory (LSTM), time delay.**

***Impact Statement*—An infectious disease pattern prediction system is developed using deterministic, stochastic, deep learning, and time delay models to investigate the impact of vaccination and population mobility on infectious disease.**

Received 26 May 2024; revised 22 July 2024 and 2 September 2024; accepted 2 September 2024. Date of publication 9 September 2024; date of current version 12 November 2024. The work of Sanjay Kumar Mohanty was supported in part by the Vellore Institute of Technology, Vellore, through the VIT SEED under Grant-RGEMS Fund SG20220069 and in part by DST-FIST Vellore under Grant-SR/FST/MS-II/2023/139-VIT. The review of this article was arranged by Editor Paolo Bonato. *(Corresponding author: Sanjay Kumar Mohanty.)*

Mohammed Salman and Sanjay Kumar Mohanty are with the School of Advanced Sciences, Vellore Institute of Technology, Vellore 632014, India (e-mail: mdsalman.molor@gmail.com; sanjaymath@gmail.com).

Pradeep Kumar Das is with the School of Electronics Engineering, Vellore Institute of Technology, Vellore 632014, India (e-mail: pdas391@gmail.com).

This article has supplementary downloadable material available at https://doi.org/10.1109/OJEMB.2024.3455801, provided by the authors.

Digital Object Identifier 10.1109/OJEMB.2024.3455801

I. Introduction

PANDEMIC simulation is a widely recognized essential tool for disease scenario analysis. Throughout history, there have been several epidemics that have had a significant impact on the evolution of society. In the past five decades, several viruses have emerged and impacted various countries and regions. Nonetheless, Covid-19 has spread remarkably around the world due to its high contagiousness and rapidity [1], [2]. Various methods are employed for this purpose, including classical ordinary differential models such as the SIR model, agent-based models, and internet-based models. The SIR model is a fundamental computational method for studying the dynamics of pandemics. The SIR model, put out by Kermack and McKendrick [3] in 1927, was one of the earliest epidemic models to be developed. Adamu et al. [4] made modifications to the SIR model by incorporating realistic assumptions to achieve a rapid decline in the infectious curve while simultaneously increasing the recovery curve. Hollingsworth [5] discussed the spread of severe acute respiratory syndrome (SARS) epidemic in 2003, which was successfully contained within a span of a year and the domain of pandemic influenza preparation, wherein mathematical models have been widely employed. Diekman et al. [6] provide a comprehensive discussion on the methodology employed to construct the next generation matrix (NGM) in order to estimate the basic reproduction number for a compartmental model. Enatsu et al. [7] established the global stability of the endemic equilibrium in an SIR model by employing a Lyapunov functional. Additionally, they demonstrated the asymptotic stability of the disease-free equilibrium. Dai et al. [8] discussed an efficient method to solve the nonlinear Volterra integral equations. Suryasa et al. [9] provided a review on Covid-19 and suggested adhering to WHO guidelines for reducing the transmission of the Covid-19 virus. These measures include maintaining a minimum distance of one meter from others, wearing a properly fitted mask, ensuring adequate ventilation by opening windows, avoiding crowded or poorly ventilated areas, practising good hand hygiene, coughing and sneezing into the elbow or disposable tissue, and receiving vaccination when eligible. In [10], [11], [12], [13], [14], the author has shown a great deal of interest in discussing various models and approaches for studying the Covid-19 epidemic in different nations. Martcheva et al. [17] proposed a mathematical model for Covid-19 pandemic to examine the effects of social distancing

on disease control and economic development. They concluded that social distancing measures can eradicate the disease, but the economy falls short of meeting the necessary social health standards. It is more probable that a combination of both social distance and health derivative is necessary. Since only a robust economy has the potential to eradicate the disease with increased social isolation.

The aforementioned approches are predominantly about deterministic mathematical models pertaining to SIR (Susceptible-Infectious-Recovered), SEIR (Susceptible-Exposed-Infectious-Recovered), or Covid-19, wherein the infection rate is regarded as a constant. There is no stochastic variation in the equations. Nevertheless, it is imperative to acknowledge that in the majority of plausible scenarios, the transmission rate of the infection is subject to stochasticity. Stochastic differential equations can provide variations of this nature. It finds applications in various fields, such as economics, there has been relatively less focus on SIR simulations. Henceforth, it is imperative to integrate the stochasticity inherent in the transmission rate within the mathematical framework. Maki and Hirose [18] presented a stochastic differential equation model as an adaptation of the SIR simulation model for the analysis of the 2003 SARS outbreak in Hong Kong. Cai et al. [19] expanded upon a traditional SIRS epidemic model by including the effects of intervention techniques on infectious forces. This was achieved by transitioning from a deterministic model to a stochastic differential equation model, which introduced random fluctuations into the system. Ríos-Gutiérrez et al. [20] focused on the study of SIR, SIS, and SEIR epidemic models employing stochastic differential equations, with a particular emphasis on stability analysis. Yang et al. [21] studied a stochastic model to explore the impact of environmental variability and Wolbachia-infected mosquitoes on dengue disease outcomes, investigating positive solutions, ergodic behaviour, and population replacement thresholds, emphasizing the influence of infected-to-uninfected mosquito ratio and environmental noise on disease control. Yu et al. [22] examined the stability of the endemic equilibrium in a model with random perturbation and found it asymptotically stable despite the stochastic perturbation. The stability condition is derived through the formulation of a Lyapunov function, and numerical simulations are subsequently presented. Gordillo et al. [23] examined a stochastic differential model that incorporates a unique reproductive term. This term combines a factor that represents the concept of an attenuated Allee effect, which has been recently proposed, with a capacity factor that regulates the size of the process.

Identification of patterns in infectious disease epidemics is crucial. It allows for a better understanding of the transmission dynamics of the disease. Early detection of disease patterns or early disease diagnosis is critical to save lives [24], [25], [26], [27]. The implementation of intervention strategies aimed at eliminating infectious diseases is contingent upon the utilization of appropriate methodologies for assessing the occurrence of outbreaks. Outbreaks in countries or provinces typically manifest at varying degrees of intensity throughout time, often influenced by factors such as seasonal fluctuations and the virus's evolutionary adaptations. The observed patterns in these settings typically have non-linear characteristics, which serves as a motivation for us to develop a system capable of capturing and modeling these non-linear dynamic changes. The utilization of non-linear systems enables us to effectively elucidate the dynamics of transmission pertaining to infectious diseases. Kim and Ahn [28] proposed SVM, SSL, and DNN models to demonstrate an effective predictive ability and forecast disease occurrences in specific countries using Medisys accumulated media data. Shahid et al. [29] evaluated various forecast models, including autoregressive integrated moving average (ARIMA), long short-term memory (LSTM), bidirectional long short-term memory (Bi-LSTM) and support vector regression (SVR). These models are examined for their effectiveness in predicting time series data related to confirmed cases, deaths, and recoveries in ten significant countries impacted by the Covid-19 pandemic. Chimmula and Zhang [30] introduced the Long short-term memory (LSTM) as a deep learning methodology for predicting future Covid-19 instances and it is anticipated that the termination of the outbreak may occur approximately in June 2020.

In an infectious disease paradigm, temporal delay is a common and normal occurrence resulting from various processes, including incubation, latency, recuperation, waning immunity, gestation, and related causes. Delay differential equations have been widely applied in numerous systems within natural science. In the field of disease modeling, several mathematical models have been developed and extensively explored over the past two decades, with a particular focus on including different types of delays. Delay differential equations are the clear and appropriate choice for modeling and incorporating these variables into a mathematical model. Delay differential equations provide a mathematical difficulty because of their intricate nature in mathematical analysis. However, they are very intriguing to mathematical modellers due to their ability to provide a more realistic depiction of dynamical systems. Das and Srivastava [31] introduced a SIR model incorporating time delay and demonstrated that the endemic equilibrium is conditionally stable under specific circumstances, whereas unstable with the presence of Hopf bifurcation. Song and Xiao [32] developed a delay differential model to investigate the influence of media on the transmission dynamics of infectious diseases with a response time of individuals to infection. Also, they examined the global bifurcation by considering the delay as a parameter to investigate Hopf bifurcations. Shayak and Sharma [33] introduce an adaptable infectious disease model using delay differential equations to effectively describe Covid-19 patterns and strategies that separate public health interventions, immune responses, and infection traits. All parameters are directly tied to the disease, enhancing prediction accuracy. Cheng and Zoa [34] have proposed a comprehensive SIRS model with a delay to thoroughly examine the dynamics of the disease. Their primary focus concerns the local bifurcation resulting from the delay parameter. They have successfully confirmed mathematically and numerically the occurrence of Hopf bifurcations. Salman et al. [35] studied a mathematical model for the Covid-19 pandemic with the effect of delay parameters on the vaccination rate.

Even though there are several machine learning, deep learning and mathematical models available for disease detection or growth prediction, there is still a need to develop a more robust infectious disease detection framework that can do both disease detection and growth prediction more accurately. It motivates us to develop a more efficient infectious disease prediction system.

A. The Contributions of the Proposed Model:

1) This study proposes a novel approach for predicting patterns of infectious diseases by combining the positive aspects of deterministic and stochastic models with those of deep learning models. Therefore, the collective advantages result in enhanced performance in the prediction of solutions.
2) The analysis of global stability at the disease free equilibrium is done effectively by the use of the Routh-Hurwitz criterion and the Lyapunov technique. On the other hand, the analysis of the endemic equilibrium in the infectious disease model is carried out using non-linear Volterra integral equations. Also, the impact of time delay on infection rates and vaccination rates is examined.
3) In contrast with existing models, this study places focus on proposing a model that is capable of examining stability while taking into account the impact of vaccination and migration rates.
4) The impact of vaccination on infection rates is thoroughly estimated through the utilization of an efficient deep-learning model that effectively captures long-term dependencies in sequential data.

Hence, this article presents a mathematical model for infectious disease that incorporates a combination of deterministic, stochastic, and delay differential equations. The model is discussed in sections 2, 3, and 5, where threshold requirements for the population are derived, and the steady-state behaviour of the system is examined for both harmless and contagious environments. In the fourth section, we discuss an artificial intelligence (AI) methodology for forecasting the number of infected individuals in the population, taking into account their vaccination status. This is achieved by utilizing the outcomes of both deterministic and stochastic models. Subsequently, the numerical results are presented to support the outcomes discussed in the preceding sections. Finally, the conclusion of the article is derived.

II. The Deterministic System

In this section, we will proceed to construct a mathematical model for an infectious disease epidemic within a population. A well-mixed population of size N at time t is assumed to be evenly distributed over four categories: susceptible(S), infectious without symptoms or asymptomatic(A), infectious with symptoms(I) and vaccinated(V) individuals. We assume each category of individuals has at least one individual initially. The individuals in category S come into physical contact with those in category A or I, causing them to become infectious whether or not they exhibit symptoms and move into category A or I, respectively. As long as the individuals remain in category V, we regard them are protected and immunized. The decline in vaccine efficacy renders them susceptible again. Also, we define the migrating individual to and fro in the total population N as constant positive rates. The deterministic system is depicted as follows:

TABLE I
PARAMETER DESCRIPTION

Parameter	Description
δ	Probability of influenza immunity of individuals in S
Λ	Birth rate
M_I	Rate for migrating population getting into the population
d	Natural death rate
λ_1	Rate for vaccination of susceptible
β	Infectious rate
p	Ratio for susceptible individuals moving to asymptomatic
γ_A	Recovery rate of individuals in A
γ_I	Recovery rate of individuals in I
λ_2	Rate for the failure of vaccination
M_O	Rate for migrating population moving out from the population
μ	Rate for identifying the individuals in A

$$\begin{aligned}
\dot{S} &= (1-\delta)\Lambda + M_I S - dS - \lambda_1 S - \beta S(I+pA) + \gamma_A A \\
&\quad + \gamma_I I + \lambda_2 V - M_O S, \\
\dot{A} &= M_I A + p\beta SA - dA - \mu A - \gamma_A A - M_O A, \\
\dot{I} &= M_I I + \beta SI + \mu A - dI - \gamma_I I - M_O I, \\
\dot{V} &= \delta\Lambda + M_I V + \lambda_1 S - dV - \lambda_2 V - M_O V, \qquad (1)
\end{aligned}$$

where $\dot{X}_j$ represent $\frac{dX_j}{dt}$, and the positive constant rates are defined in Table I.

It is assumed that the sum of the migration out rate and natural death rate is always greater than the migration in rate, let $\psi = d + M_O - M_I$, i.e. $\psi > 0$. From the system (1), it follows that the total population $N(t)$ can be defined as

$$N(t) = S(t) + A(t) + I(t) + V(t), \qquad (2)$$

implies

$$\frac{dN}{dt} = \Lambda - \psi N, \qquad (3)$$

then

$$N(t) = \frac{\Lambda}{\psi}. \qquad (4)$$

From (4), we get $N(t)$ is bounded, and all the categories of individuals are bounded as well, as they are all non-negative and sum up to N. Then the global attractor for the system (1) is

given as

$$\Gamma_1 = \left\{ (S, A, I, V) \in \mathbf{R}_+^4 : S + A + I + V = \frac{\Lambda}{\psi} \right\}. \quad (5)$$

It is easy to verify that 'Γ_1' is positively invariant. A system reaches equilibrium when the disease either completely eradicates itself from the population or continues to exist there at a steady level. On setting the derivatives of all compartments to zero, the equilibria are determined by solving the obtained system of equations for S, A, I, and V using (2) and (3). We now discuss the possible equilibria for the system (1) in two subsections.

In the following subsection, we examine the disease free equilibrium of the system (1), the threshold parameter known as the basic reproduction number and how its value affects the stability of disease free equilibrium, which aids in infection control strategies.

A. The Harmless Environment

In this section, we first obtain the disease free equilibrium of the system (1), then we discuss the derivation of basic reproduction number, and the local as well as global stability of disease free equilibrium in two subsubsections. The disease free equilibrium is one of two possible equilibria of the system (1), and it is obtained as

$$E_D = (S_D, A_D, I_D, V_D), \quad (6)$$

with

$$S_D = \frac{\Lambda(\psi(1-\delta)+\lambda_2)}{\psi(\psi+\lambda_1+\lambda_2)}, \quad A_D = 0,$$
$$I_D = 0, \quad V_D = \frac{\Lambda(\psi\delta+\lambda_1)}{\psi(\psi+\lambda_1+\lambda_2)}.$$

Further, we utilize the disease free equilibrium (6) stated above to derive the basic reproduction number.

The basic reproduction number($\mathcal{R}_0$) is the standard definition of secondary infection in epidemiology, and it represents the average number of new cases caused by the introduction of a single infectious individual(with or without symptoms) into a community of susceptible individuals. For the system (1), we use the approach described in Van den Driessche [36], which involves calculating $\mathcal{R}_0$ from the next generation matrix($\mathtt{FV}^{-1}$). The matrix '$\mathtt{F}$' and matrix '$\mathtt{V}$' represents the Jacobian of the collection of rates involving infectious transmission($\mathcal{F}_k$) and the collection of other transmissions between compartments($\mathcal{V}_k$) at disease free equilibrium (1), respectively. The collections $\mathcal{F}_k$ and $\mathcal{V}_k$ are obtained by recasting the system (1) as

$$\frac{dX_k}{dt} = \mathcal{F}_k - \mathcal{V}_k, \quad k = 1, 2, \quad (7)$$

where 'X_1' denote the category A, and 'X_2' denote the category I. Hence, the matrix $\mathtt{F}$, $\mathtt{V}$ and $\mathtt{FV}^{-1}$ are obtained as

$$\mathtt{F} = \begin{bmatrix} pf_1 & 0 \\ 0 & f_1 \end{bmatrix}, \quad \text{with } f_1 \text{ as } \frac{\beta\Lambda(\psi(1-\delta)+\lambda_2)}{\psi(\psi+\lambda_1+\lambda_2)}, \quad (8)$$

$$\mathtt{V} = \begin{bmatrix} \psi+\mu+\gamma_A & 0 \\ -\mu & \psi+\gamma_I \end{bmatrix}, \quad (9)$$

and

$$\mathtt{FV}^{-1} = \begin{bmatrix} m_{11} & m_{12} \\ m_{21} & m_{22} \end{bmatrix}, \quad (10)$$

with

$$m_{11} = \frac{\beta\Lambda p(\psi(1-\delta)+\lambda_2)}{\psi(\psi+\lambda_1+\lambda_2)(\psi+\mu+\gamma_A)}, \quad m_{12} = 0,$$
$$m_{21} = \frac{\beta\Lambda(\psi(1-\delta)+\lambda_2)\mu}{\psi(\psi+\lambda_1+\lambda_2)(\psi+\mu+\gamma_A)(\psi+\gamma_I)},$$
$$m_{22} = \frac{\beta\Lambda(\psi(1-\delta)+\lambda_2)}{\psi(\psi+\lambda_1+\lambda_2)(\psi+\gamma_I)}.$$

Therefore, on deriving the spectral radius of $\mathtt{FV}^{-1}$ in (10), we get $\mathcal{R}_0$ as

$$\mathcal{R}_0 = \frac{\Lambda\beta p(\psi(1-\delta)+\lambda_2)}{\psi(\psi+\lambda_1+\lambda_2)(\psi+\mu+\gamma_A)}. \quad (11)$$

The following subsection is established to prove the local stability of disease free equilibrium (6).

1) Local Stability of Disease Free Equilibrium: This subsection contains the result to prove the local stability of disease free equilibrium (6) of the system (1) using Routh-Hurwitz criteria. It is a mathematical technique through an algebraic approach to check whether the roots of the polynomials are in the left half plane. This technique is frequently used to determine the stability of the system. Also, without directly calculating roots, the coefficients of characteristic equations are analysed. The following lemma states the necessity of parameters for the stability of disease free equilibrium (6) of the system (1).

Lemma 1: Assume that the system (1) satisfies the following conditions:

$$\beta p(1+\Lambda\psi\delta+\lambda_1) > \frac{\psi(\psi+\mu+\gamma_A)}{\psi+\lambda_1+\lambda_2},$$
$$\frac{\psi+\mu+\mu\beta p}{\psi+\lambda_1+\gamma_I} = \frac{\psi+\lambda_2+\mu\beta}{\psi+\lambda_1+\lambda_2} = \psi+\mu+\gamma_A, \quad (12)$$

then the disease free equilibrium (6) of the system (1) is locally asymptotically stable if $\mathcal{R}_0 < 1$, and unstable if $\mathcal{R}_0 > 1$.

Proof: Proof is provided in Supplementary Materials VII-A. □

The next subsubsection is established to prove the results of global stability of disease free equilibrium (6) of the system (1).

2) Global Stability of Disease Free Equilibrium: In this subsubsection, we follow the Lyapunov method to prove the global stability of disease free equilibrium (6) of the system (1) through the lemma stated below. For simplicity, here we consider the following notions:

$\alpha_1 = \psi$, $\alpha_2 = \Lambda\beta p(\alpha_1(1-\delta)+\lambda_2)$, $\alpha_3 = \alpha_1+\lambda_1+\lambda_2$, $\alpha_4 = \alpha_1+\mu+\gamma_A$ and $\alpha_5 = \alpha_1+\gamma_I$.

Lemma 2: If $\mathcal{R}_0 < 1$, the disease free equilibrium (6) of system (1) is globally asymptotically stable with assumption, $\alpha_2 > \alpha_1\alpha_3(p\beta S + \alpha_4)$.

Proof: Proof is provided in Supplementary Materials VII-B. □

In the next subsection, we focus on another equilibrium of the system (1), known as endemic equilibrium and its stability.

B. The Contagious Environment

In this subsection, we present the existence of endemic equilibrium of the system (1) and to examine the local stability of endemic equilibrium [37]. The endemic equilibrium will have a positive count of individuals in infectious categories. The system (1) has disease free equilibrium (6) as discussed in the previous subsection. Also, the system (1) allows for the endemic equilibrium, if the following conditions are met:

$$\frac{\psi+\mu+\gamma_A}{\psi+\gamma_I} < p < \frac{(\psi+\lambda_1+\lambda_2)\psi(\gamma_A+\psi+\mu)}{(\lambda_2+(1-\delta)\psi)\beta}$$

and $\mathcal{R}_0 > 1$. The endemic equilibrium of system (1) is obtained as

$$E_E = (S_E, A_E, I_E, V_E), \tag{13}$$

with

$$S_E = \frac{\psi+\mu+\gamma_A}{\beta p},$$

$$I_E = \frac{p\mu A_E}{p(\psi+\gamma_I)-(\psi+\mu+\gamma_A)},$$

$$V_E = \frac{\Lambda\delta\beta p+\lambda_1(\psi+\mu+\gamma_A)}{\beta p(\psi+\lambda_2)},$$

$$A_E = \left(\frac{\alpha_3(\gamma_A+\psi+\mu)}{\beta p(\lambda_2+\psi)R_0}\right)(\alpha_3\psi(\gamma_A+\psi+\mu)(R_0-1) + \beta p(\lambda_2+(1-\delta)\psi),$$

where $\alpha_3 = \psi+\lambda_1+\lambda_2$. Consequently, it is noticeable that $\mathcal{R}_0$ must be greater than one for the existence of endemic equilibrium (13). To study the stability of endemic equilibrium (13) of the system (1), if the disease free equilibrium (6) is unstable for some coditions as in lemma (1) and lemma (2), we transform the system (1) into Volterra Integral Equation in the following subsubsection.

1) Nonlinear Integral Equation for Deterministic System:

Here, we establish the results that prove the local stability of the endemic equilibrium (13) of the system (1) by changing the system (1) into integral equations and transforming the endemic equilibrium (13) of the system (1) to the origin (0,0,0) of Volterra Integral Equation. The system (1) is suitable for short-term forecast and analysis, since it prioritizes the current state over the past input history. Volterra integral equations are very suitable for the representation of systems that exhibit memory effects, wherein the present state is influenced not only by the current input but also by previous inputs. Volterra integral equations have the inherent capability to effectively address nonlinear systems, rendering them suitable for modeling systems exhibiting nonlinear behaviour. The transformation of system (1) into integral equations is as follows:

First, let us look at the categories A, I, and V. Then, we use them to obtain the category S. Consider the following:

$$x(t-s) = e^{-(\psi+\mu+\gamma_A)(t-s)}, \quad y(t-s) = e^{-(\psi+\gamma_I)(t-s)},$$

and $z(t-s) = e^{-(\psi+\lambda_2)(t-s)}$.

Using $x(t-s)$, $y(t-s)$ and $z(t-s)$, one can easily derive the equivalent form of the system (1) into following integral equations :

$$A(t) = A(0)e^{-(\psi+\mu+\gamma_A)t} + p\int_0^t x(t-s)\beta_1(s)(S(s)+\theta V(s))ds, \tag{14}$$

$$I(t) = I(0)e^{-(\psi+\gamma_I)t} + \int_0^t y(t-s)\beta_2(s)(S(s)+\theta V(s))ds + \mu\int_0^t y(t-s)A(s)ds, \tag{15}$$

$$V(t) = V(0)e^{-(\psi+\lambda_2)t} + \frac{\delta\Lambda}{\psi+\lambda_2}\left(1-e^{-(\psi+\gamma_I)t}\right) + \lambda_1\int_0^t z(t-s)S(s)ds. \tag{16}$$

The endemic equilibrium (13) of system (1) is transfered to the origin (0,0,0) of the (14)–(16) by setting

$$S(t) = \tilde{S}(t) + S_E, A(t) = \tilde{A}(t) + A_E,$$
$$I(t) = \tilde{I}(t) + I_E \text{ and } V(t) = \tilde{V}(t) + V_E.$$

Also, using the (2) and (4) the individuals in category S can be obtained as

$$\begin{aligned} S(t) &= \frac{\Lambda}{\psi} - A(t) - I(t) - V(t) \\ &= \frac{\Lambda}{\psi} - \tilde{A}(t) - \tilde{I}(t) - \tilde{V}(t) - A_E - I_E - V_E \\ &= S_E - \tilde{A}(t) - \tilde{I}(t) - \tilde{V}(t). \end{aligned}$$

Further for simplicity, the signs $\tilde{S}(t)$, $\tilde{A}(t)$, $\tilde{I}(t)$ and $\tilde{V}(t)$ are considered as $S(t)$, $A(t)$, $I(t)$ and $V(t)$, respectively. Then the integral (14)–(16) becomes

$$\begin{aligned} A(t) = &-A_E + A(0)e^{-(\psi+\mu+\gamma_A)t} + p\beta\int_0^t x(t-s)S_E A_E ds \\ &+ p\beta\int_0^t x(t-s)\left(A(s)\left(S_E - A(s) - I(s) - V(s)\right)\right. \\ &\left. -A_E(A(s)+I(s)+V(s))\right)ds, \end{aligned} \tag{17}$$

$$\begin{aligned} I(t) = &-I_E + I(0)e^{-(\psi+\gamma_I)t} + \mu\int_0^t y(t-s)A_E ds \\ &+ \beta\int_0^t y(t-s)I_E S_E ds + \beta\int_0^t \left(I(s)\left(S_E - A(s)\right)\right. \\ &\left. -I(s) - V(s) - I_E(A(s)+I(s)+V(s))\right)ds \\ &+ \mu\int_0^t y(t-s)A(s)ds + \beta\int_0^t y(t-s)ds, \end{aligned} \tag{18}$$

$$V(t) = -V_E + \frac{\delta\Lambda + \lambda_1 S_E}{\psi + \lambda_2} + \left(V(0) - \frac{(\delta\Lambda + \lambda_1 S_E)}{\psi + \lambda_2}\right) \times e^{-(\psi+\lambda_2)t} - \lambda_1 \int_0^t z(t-s)(A(s)+I(s)+V(s))ds. \tag{19}$$

Since A_E, I_E and V_E holds true for

$$A_E = \beta p \int_{-\infty}^{-t} A_E S_E x(-\tau_1) d\tau_1,$$

$$I_E = \int_{-\infty}^{-t} (\beta I_E S_E + \mu A_E)\, y(-\tau_1) d\tau_1,$$

$$V_E = \frac{\delta\Lambda + \lambda_1 S_E}{\psi + \lambda_2},$$

the integral (17)–(19) can be changed to a nonlinear Volterra integral equation as follows:

$$Y(t) = U(t) + \int_0^t V(t-s) W(Y(s)) ds, \tag{20}$$

where $Y(t) = \begin{bmatrix} A \\ I \\ V \end{bmatrix}$, $U(t) = \begin{bmatrix} u_1(t) \\ u_2(t) \\ u_3(t) \end{bmatrix}$, $V(t) = \begin{bmatrix} x(t) & 0 & 0 \\ 0 & y(t) & 0 \\ 0 & 0 & z(t) \end{bmatrix}$ and $W(s) = \begin{bmatrix} W_1(s) \\ W_2(s) \\ W_3(s) \end{bmatrix}$,with

$$u_1(t) = A(0)e^{-(\psi+\mu+\gamma_A)t} - \beta p \int_{-\infty}^{-t} A_E S_E x(-\tau_1) d\tau_1,$$

$$u_2(t) = I(0)e^{-(\psi+\gamma_I)t} - \int_{-\infty}^{-t} (\beta I_E S_E + \mu A_E)\, y(-\tau_1) d\tau_1,$$

$$u_3(t) = \left(V(0) - \frac{(\delta\Lambda + \lambda_1 S_E)}{\psi + \lambda_2}\right) e^{-(\psi+\lambda_2)t},$$

and

$$W_1(Y(s)) = \beta p A(s)\,(S_E - A(s) - I(s) - V(s)) - \beta p A_E (A(s) + I(s) + V(s)),$$

$$W_2(Y(s)) = \beta I(s)\,(S_E - A(s) - I(s) - V(s)) - \beta I_E (A(s) + I(s) + V(s)) + \mu A(s),$$

$$W_3(Y(s)) = -\lambda_1 (A(s) + I(s) + V(s)).$$

The following subsubsection discusses the asymptotic stability of (0,0,0) of the non-linear Volterra integral (20).

2) Asymptotic Stability of Endemic Equilibrium: In this subsubsection, our focus is on examining the asymptotic stability of the endemic equilibrium (13) of the system (1). This analysis relies upon the asymptotic stability of the origin (0,0,0) in the non-linear Volterra integral (20). We now established a result to prove the asymptotic stability of (0,0,0) of the non-linear Volterra integral (20).

Theorem 1: If the solutions of the non-linear Volterra integral (20) are bounded and lies on $[0,\infty), U(t) \in C[0,\infty), U(t) \to 0$ as $t \to \infty, V(t) \in L^l[0,\infty), W(X) \in C^1(\mathbf{R}^2), W(0) = 0$, the Jacobian matrix of W at (0,0,0) is nonsingular, and the characteristic polynomial with I_m as identity is

$$\left| I_m - \int_0^\infty e^{-\lambda t} V(t) J_W \right| = 0, \tag{21}$$

then (0,0,0) is locally asymptotically stable for the non linear Volterra integral (20).

Proof: Proof is provided in Supplementary Materials VII-C. □

Remark: The results and discussion from subsection (2.1)–(2.2), summarize that the disease-free equilibrium (6) of system (1) is stable with $\mathcal{R}_0 < 1$ and the endemic equilibrium (13) of system (1) is stable with $\mathcal{R}_0 > 1$.

In the subsequent section, a perturbation term is incorporated into the system (1) to establish a stochastic system.

III. Stochastic System

This section examines the stochastic system, a variant of the deterministic system (1). It is essential to study associated stochastic systems in order to comprehend the dynamics of the system (1), as the infectious rate changes over time in reality. Stochastic systems account for the inherent randomness and uncertainty in disease transmission. By simulating multiple possible outcomes, stochastic systems can provide a more accurate picture of how a disease might spread and evolve. However, stochastic systems are also more complex and computationally intensive than the associated deterministic systems. Despite these challenges, stochastic systems have become an increasingly important tool in research, helping policymakers to make informed decisions about disease control and prevention strategies. An associated stochastic system is formed by the introduction of a perturbation parameter that affects the infection rate of the S, A, and I categories in the system (1), and is given as

$$\begin{aligned} dS &= ((1-\delta)\Lambda + M_I S - dS - \lambda_1 S - \beta S(I + pA) + \gamma_A A \\ &\quad + \gamma_I I + \lambda_2 V - M_O S)\, dt - \sigma S(I + pA) dW(t), \\ dA &= (M_I A + p\beta SA - dA - \mu A - \gamma_A A - M_O A) dt \\ &\quad + p\sigma SA dW(t), \\ dI &= (M_I I + \beta SI + \mu A - dI - \gamma_I I - M_O I) dt + \sigma SI dW(t), \\ dV &= (\delta\Lambda + M_I V + \lambda_1 S - dV - \lambda_2 V - M_O V) dt, \end{aligned} \tag{22}$$

with 'σ' as the perturbation parameter related to the infectious rate, '$W(t)$' is a Weinear process, and all the positive constants are the same as in the system (1). When the parameter 'σ' equals zero, then the stochastic system simplifies to a deterministic system. Hence, the analysis performed for the deterministic system will be applied since it is no longer a stochastic system. Since most of the real-world scenarios are stochastic in nature, we assume a positive value for 'σ'.

Next, we discuss the stability of disease free equilibrium (6) for the stochastic system (22).

Theorem 2: Let $\mathcal{R}_0$ and disease free equilibrium be same as in system (1), if

$$\mathcal{R}_0 < \frac{1}{(\psi+\mu+\gamma_A)A}, \quad \frac{\beta S}{\psi+\gamma_I} < 1 < \frac{p\beta S}{\psi+\mu+\gamma_A},$$
$$\text{and } \beta SI > A\mu + (\psi+\gamma_I)I,$$

then disease free equilibrium (6) is asymptotically stable for system (22) with appropriately small $\sigma > 0$.

Proof: Proof is provided in Supplementary Materials VII-D. □

In the subsequent subsection, our exclusive attention is directed towards examining the relation between the solutions of category I and category V with the intent of training through the neural network.

IV. Deep Learning Based Prediction

In this section, an efficient framework is proposed to improve the prediction performance by integrating mathematical models and neural networks. The deterministic system (1) and stochastic system (22) demonstrate favourable performance, but there remains potential for further enhancements. The advancement of deep learning motivates us to leverage the advantages offered by deep learning models, specifically employing Long Short-Term Memory (LSTM) networks on the obtained solution from the proposed mathematical model. We now focus on solutions of the system (1) and (22) for category I and category V; we use LSTM to forecast the number of individuals in category I based on the number of individuals in category V. Since LSTM networks have proven to be highly effective in capturing long-term dependencies in sequential data. Understanding the mathematical principles underlying LSTM networks enables us to exploit their capabilities for tasks involving time series data, thereby facilitating improved performance [39].

The LSTM architecture is composed of interconnected memory cells that enable the storage and retrieval of information over extended periods. Its main components consist of the input gate, forget gate, output gate, and memory cell [40]. The input gate determines the importance of new input in relation to the current state of the LSTM cell, controlling the information flow and cell state update. The activation of the input gate is calculated as follows:

$$i_t = \sigma(W_i * [h_{t-1}, x_t] + b_i), \tag{23}$$

where i_t represents the input gate activation at time t, σ denotes the sigmoid activation function, W_i corresponds to the weight matrix of the input gate, h_{t-1} refers to the previous hidden state, x_t represents the current input, and b_i is the bias term for the input gate.

The forget gate determines the extent to which previously stored information should be disregarded, governing the retention or removal of information from the memory cell. The activation of the forget gate is computed as follows:

$$f_t = \sigma(W_f * [h_{t-1}, x_t] + b_f), \tag{24}$$

where f_t denotes the forget gate activation at time t, W_f represents the weight matrix for the forget gate, h_{t-1} denotes the previous hidden state, x_t represents the current input, and b_f corresponds to the bias term for the forget gate.

The memory cell stores the acquired information from the input sequence and updates the cell state at each time step. By combining the input gate and forget gate information, the memory cell state is updated as follows:

$$C_t = f_t * C_{t-1} + i_t * \tanh(W_C * [h_{t-1}, x_t] + b_C), \tag{25}$$

where C_t represents the updated memory cell state at time t, C_{t-1} represents the previous memory cell state, W_C denotes the weight matrix for the memory cell, $\tanh$ refers to the hyperbolic tangent activation function, and b_C corresponds to the bias term for the memory cell.

The output gate determines the relevance of the current memory cell state to the hidden state and generates the output for the current time step. It controls the information flow from the memory cell to the output. The activation of the output gate is calculated as follows:

$$o_t = \sigma(W_o * [h_{t-1}, x_t] + b_o), \tag{26}$$

where o_t denotes the output gate activation at time t, W_o represents the weight matrix for the output gate, h_{t-1} denotes the previous hidden state, x_t represents the current input, and b_o corresponds to the bias term for the output gate. We next move on to discuss the mathematical system with the time delay parameter associated to the system (1).

V. The Delayed System

In this section, we present the time delay systems associated with the system (1). Adding delays to epidemic models has assisted researchers in better comprehending the complexities involved in illustrating the dynamics of infectious diseases. Latent period inclusion is the primary focus on delayed systems in epidemic models. This assumes that the total number of infections in earlier times determines the current infectious rate. Since time delays can alter the qualitative characteristics of the system, such as destabilizing an equilibrium and so leading to periodic solutions via Hopf bifurcation, epidemic models with time delays require considerable attention. The time delay systems associated with the system (1) are formulated by dividing into two distinct time delay systems, one with a time delay in infectious rate and another with a time delay in vaccination-related rates. Both the time delay systems are discussed in two subsections.

A. Time Delay System With Delay in Infectious Rate

Here, we introduce a time delay parameter associated with the infectious rate, and we focus on the S, A, and I categories. The time delay is indicated by the parameter '$\tau > 0$'. Below is a description of the time delay system that includes a delay parameter associated with the infectious rate in the S, A, and I categories.

$$\frac{dS}{dt} = (1-\delta)\Lambda + M_I S - dS - \lambda_1 S - \beta S(I(t-\tau) + pA(t-\tau)) + \lambda_2 V - M_O S,$$

$$\frac{dA}{dt} = M_I A + p\beta SA(t-\tau) - dA - \mu A - M_O A,$$
$$\frac{dI}{dt} = M_I I + \beta SI(t-\tau) + \mu A - dI - M_O I, \quad (27)$$

where the positive constants are the same as in system (1). It is crucial to define the value of the solution prior to $t = 0$ with an initial condition. In this case, the initial conditions are $S_0(\theta) = \phi_1(\theta) > 0$, $A_0(\theta) = \phi_2(\theta) > 0$, $I_0(\theta) = \phi_3(\theta) > 0$, with $\theta \in [-\tau, 0]$, where $\phi_i \in C([-\tau, 0] \to \mathbb{R}_+)$, $(i = 1, 2, 3)$ are given functions. Similar to the global attractor (5) of the system (1), the biologically feasible region for the delayed system (27) is obtained as

$$\Gamma_2 = \left\{(S, A, I) \in \mathbb{R}^3_+ : S, A, I \geq 0\right\}, \quad (28)$$

and also, following the discussion related to the global attractor (5) of the system (1), 'Γ_2' is positively invariant. The two required equilibria of system (27) are defined as disease free equilibrium ($E_{D*} = (S_{D*}, A_{D*}, I_{D*})$) and endemic equilibrium ($E_{E*} = (S_{E*}, A_{E*}, I_{E*})$).

Now, the following theorem is established to prove the asymptotic stability of disease free equilibrium ($E_{D*} = (S_{D*}, A_{D*}, I_{D*})$) of the system (27).

Theorem 3: The disease free equilibrium ($E_{D*} = (S_{D*}, A_{D*}, I_{D*})$) of the system (27) is linearly asymptotically stable for $\tau \geq 0$ with some constants $K_i > 0$, $i = 1, 2, 3$.

Proof: Proof is provided in Supplementary Materials VII-E. □

In the following section, we provide a brief discussion about the bifurcation of the endemic equilibrium ($E_{E*} = (S_{E*}, A_{E*}, I_{E*})$) of the system (27).

1) Hopf Bifuraction: We now discuss the stability and the Hopf bifurcation of the endemic equilibrium ($E_{E*} = (S_{E*}, A_{E*}, I_{E*})$) of the system (27). Hopf bifurcation is a significant type of bifurcation observed in the study of dynamical systems, it signifies a fundamental shift in the behaviour of a system. At a specific critical value of the time delay parameter, the stability of the equilibrium point undergoes a transition from stability to instability. Here we consider the delay 'τ^*' to be the critical time delay at which bifurcation occurs and the Theorem (3) holds true for the endemic equilibrium ($E_{E*} = (S_{E*}, A_{E*}, I_{E*})$) of the system (27). Contrary assuming that the characteristic polynomial (49) does not satisfy the Routh-Hurwitz criteria with $K_3 < 0$, the characteristic polynomial (49) has one positive root and a pair of imaginary roots. Then, from this endemic equilibrium ($E_{E*} = (S_{E*}, A_{E*}, I_{E*})$) of the system (27), periodic solutions bifurcate as 'τ' passes through the critical value. The critical time delay 'τ^*' is obtained by solving the transcendental (50)–(51) as

$$\tau^* = \frac{1}{2z} \arccos\left[\frac{D_1 z^2\left(\omega^{*2} - U_2\right) + D_2\left(z^2 B_1 - B_3\right)}{z^2 B_1^2 + B_2^2}\right] + \frac{2n\pi}{z}, n = 0, 1, 2, \cdots \quad (29)$$

At $x = iz$, $\tau = \tau^*$ with $2z^2(B_3 - B_1 z^2) > 0$, it is seen that

$$\left[\frac{d(\mathrm{Re}(x))}{d\tau}\right] > 0. \quad (30)$$

From the (29)–(30), we conclude that the endemic equilibrium ($E_{E*} = (S_{E*}, A_{E*}, I_{E*})$) of the system (27) is stable for $\tau \in [0, \tau^*)$ and unstable for $\tau > \tau^*$ [41]. Next, we establish the following subsection to discuss another time delay system in which the time delay parameter is associated with vaccination-related rates.

B. Time Delay System With Delay in Vaccination-Related Rates

We now introduce a time delay parameter associated with the vaccination rate and the failure of the vaccination rate to obtain precise results on S and V categories. Here, the time delay is indicated by the parameter '$\tau_1 > 0$'. Below is a description of the time delay system that includes a delay parameter associated with the vaccination rate and the failure of the vaccination rate in the S and V categories.

$$\frac{dS}{dt} = (1-q)\Lambda + M_I S - pS(t-\tau_1) - \lambda_1 S + \lambda_2 V(t-\tau_1) - M_O S,$$
$$\frac{dV}{dt} = q\Lambda + M_I V + \lambda_1 S(t-\tau_1) - pV - \lambda_2 V(t-\tau_1) - M_O V, \quad (31)$$

where the positive constants are the same as in system (1). It is crucial to define the value of the solution prior to $t = 0$ with an initial condition. In this case, the initial conditions are $S_0(\theta) = \phi_1(\theta) > 0, V_0(\theta) = \phi_2(\theta) > 0$, with $\theta \in [-\tau, 0]$, where $\phi_i \in C([-\tau, 0] \to \mathbb{R}_+), \quad i = 1, 2$, are given functions. Similar to the global attractor (5) of the system (1), the feasible region for the delayed system (31) is obtained as

$$\Gamma_3 = \left\{(S, V) \in \mathbb{R}^2_+ : S, V \geq 0\right\}, \quad (32)$$

and also, following the discussion related to the global attractor (5) of the system (1), 'Γ_3' is positively invariant. The positive equilibrium of (31) is defined as $E_* = (S_*, V_*)$. Now, the following theorem is established to prove the asymptotic stability of equilibrium ($E_* = (S_*, V_*)$) of the system (31).

Theorem 4: The equilibrium ($E_* = (S_*, V_*)$) of the system (31) is linearly asymptotically stable for $\tau_1 \geq 0$.

Proof: Proof is provided in Supplementary Materials VII-F.□

Remark: The critical time 'τ_1^*' by solving the transcendental (55)–(56), similar to previous subsection as

$$\tau_1^* = \frac{1}{z^*} \arccos\left[\frac{(V_2 W_2 - V_2 z^{*2} + V_1 W_1 z^{*2})}{W_1^2 z^{*2} + B_2^2}\right]. \quad (33)$$

The Hopf bifurcation occurs at τ_1^*. Hence, the equilibrium ($E_*(S_*, V_*)$) of the system (31) is stable for $\tau_1 \in [0, \tau_1^*)$ and unstable for $\tau_1 > \tau_1^*$. Now, we proceed with numerical examples to better understand the proposed mathematical systems.

VI. Numerical Simulations

This section focuses on the numerical simulation of the mathematical systems discussed in the sections that followed. The objective is to analyze the impact of two major control strategies of an epidemic, that is, vaccination and migration, on individuals

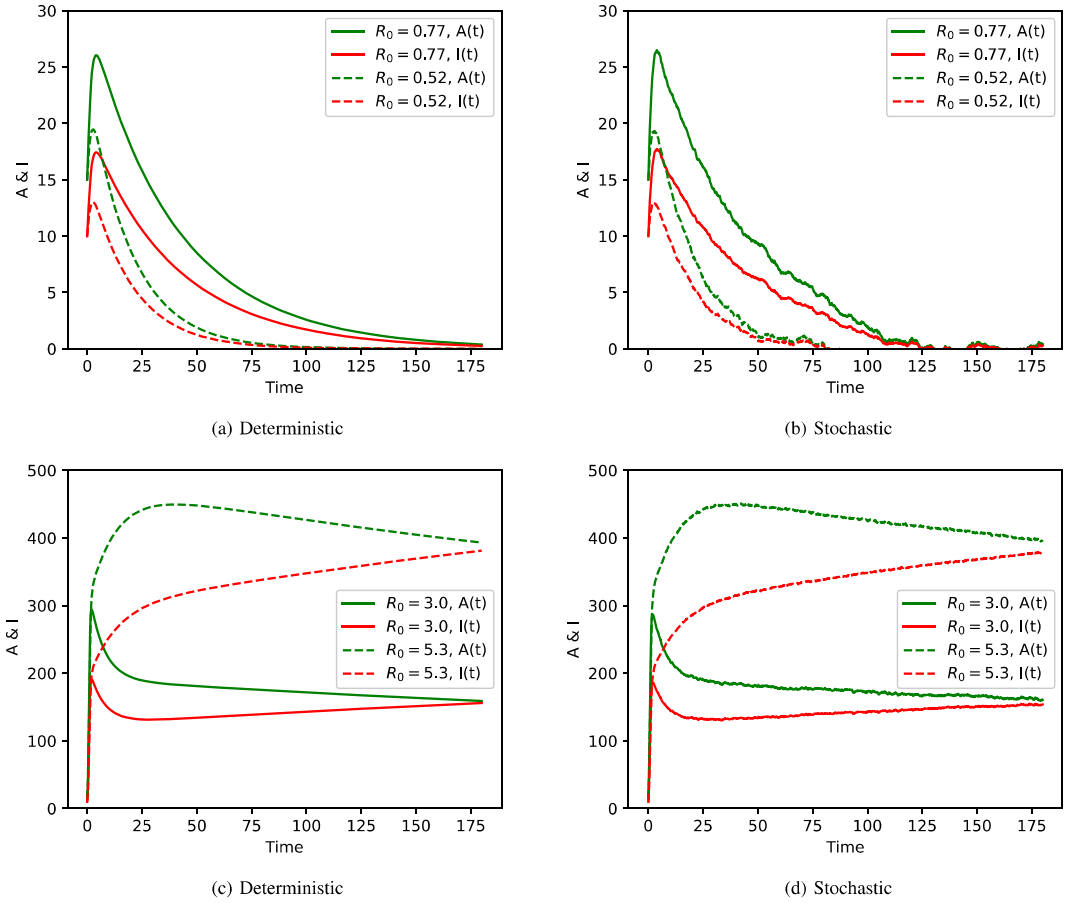

(a) Deterministic (b) Stochastic

(c) Deterministic (d) Stochastic

Fig. 1. Total individuals in categories A and I of the system (1)–(22). Fig. 1(a)–(b) are with $R_0 < 1$, $\Lambda = 100$, $M_1 = 0.5$, $M_2 = 0.6$, $\delta = 0.05$, $\beta = 0.006$ & 0.004, $\lambda_1 = 0.6$, $\mu = 0.0001$, $\gamma_A = 0.004$, $\gamma_I = 0.005$, $\lambda_2 = 0.0006$, $d = 0.0001$ and $\sigma = 1.03093 \times 10^{-5}$. Fig. 1(c) and (d) are with $R_0 > 1$, $\Lambda = 100$, $M_1 = 1$ & 0.6, $M_2 = 1.2$ & 0.7, $\delta = 0.05$, $\beta = 0.005$ & 0.004, $\lambda_1 = 0.6$, $\mu = 0.002$, $\gamma_A = 0.001$, $\gamma_I = 0.001$, $\lambda_2 = 0.0006$, $d = 0.0001$ and $\sigma = 1.03093 \times 10^{-5}$.

categorized as A and I. Additionally, we observe that the value of $\mathcal{R}_0$ has an impact on the trajectory of the infectious curve obtained from the system (1) and (22), either amplifying or attenuating its growth. We investigate the impact of the time delay parameter on the number of individuals in category I derived from system (27) and the role of time delay associated with vaccination rate and failure of vaccination rate derived from system (31). To identify the optimal parameters, it is essential to use historical data and statistical methods for their accurate estimation. We fix the total population with 1000 individuals. Initially, we consider the number of individuals in categories S, A, I, and V is 970, 15, 10, and 5, respectively.

Fig. (1) depicts the influence of $\mathcal{R}_0$ on the populations affected by the infectious disease, both in category A and category I. It is evident from Fig. 1(a) and (c) that when $\mathcal{R}_0$ is less than one, the number of individuals in both category A and category I tend to converge towards the disease free equilibrium (6). Furthermore, the maximum number of individuals in both categories does not exceed twenty-six. Conversely, when $\mathcal{R}_0$ exceeds one, the number of infected individuals in both category A and category I surpasses twenty-six very fast and converges to endemic equilibrium(13). Additionally, the stability analysis reveals that the disease free equilibrium is stable for values of $\mathcal{R}_0$ less than one, while an endemic equilibrium state exists and remains stable for values of $\mathcal{R}_0$ greater than one. Hence, for lower values of $\mathcal{R}_0$, the number of individuals in category A or I diminishes within a short timeframe, while for higher values of $\mathcal{R}_0$, the number of individuals in category A or I persists indefinitely without reaching zero after a certain period. In Fig. 1(b) and (d), the number of individuals in category A and category I, under the influence of minor random fluctuations, are shown. It is seen that when $\mathcal{R}_0 < 1$ and $\mathcal{R}_0 > 1$, the stochastic system (22) fluctuates around the deterministic system (1), indicating random variation without significant outbreaks. These results highlight the significance of integrating deterministic and stochastic approaches to disease dynamics, as they provide insight into both short and long-term behaviours and the impact of random fluctuations on disease outbreaks.

Figs. 2–3 illustrates the changes in the number of individuals in category I and category V over time in system (1)–(22), considering different rates of vaccination success and failure. In Fig. 2(a), the vaccination rate exhibits variation while maintaining fixed values for the vaccine failure rate. Conversely, in Fig. 2(b), the vaccine failure rate demonstrates variation while keeping the vaccination rate constant. The results show that as the vaccination rate increases, there is a corresponding decrease

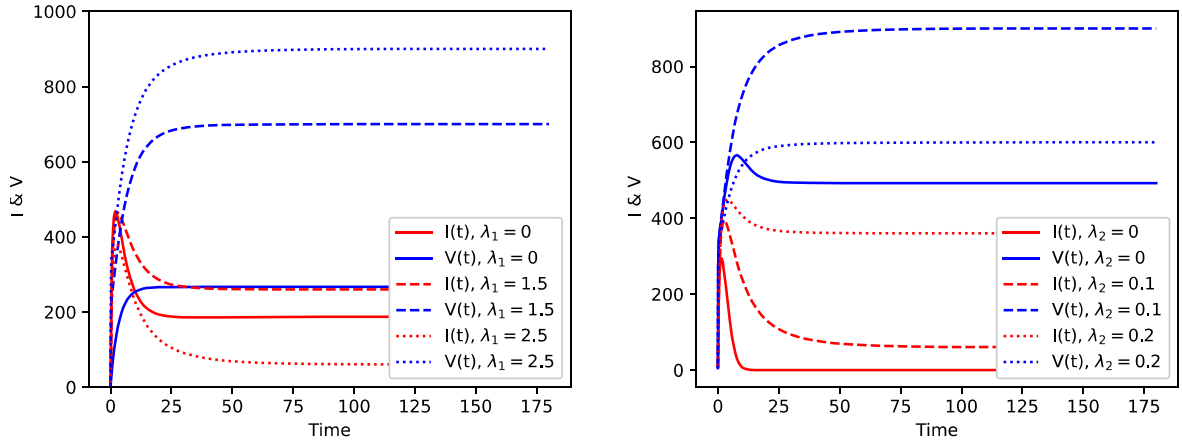

(a) Various λ_1 with $\lambda_2 = 0.1$ (b) Various λ_2 with $\lambda_1 = 2.5$

Fig. 2. Effect of λ_1 and λ_2 on category I and V of the system (1) with $\Lambda = 100$, $M_1 = 1.1$, $M_2 = 1.2$, $\delta = 0.8$, $\beta = 0.02$, $\mu = 0.8$, $\gamma_A = 0.3$, $\gamma_I = 0.7$ and $d = 0.1$.

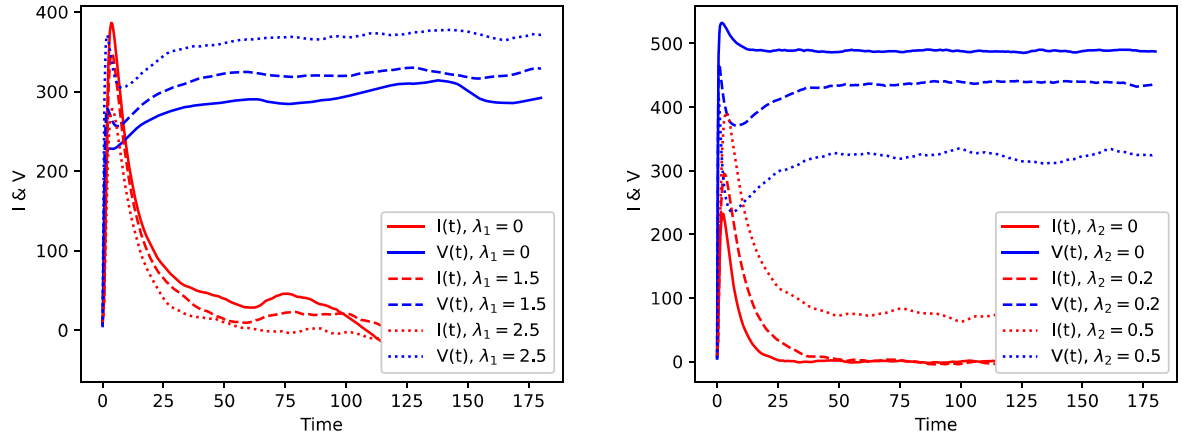

(a) Various λ_1 with $\lambda_2 = 0.1$ (b) Various λ_2 with $\lambda_1 = 2.5$

Fig. 3. Effect of λ_1 and λ_2 on category I and V of the system (22) with $\Lambda = 100$, $M_1 = 1.1$, $M_2 = 1.2$, $\delta = 0.8$, $\beta = 0.001$, $\mu = 0.8$, $\gamma_A = 0.0001$, $\gamma_I = 0.0001$, $d = 0.1$ and $\sigma = 5.15464 \times 10^{-5}$.

in the number of individuals in category I. Therefore, in order to effectively prevent infections within the population, it is crucial to maintain a high vaccination rate and minimize the rate of vaccination failures. The following Fig. 4(a)–(b), depict the LSTM model that has been trained using data representing solutions from both deterministic and stochastic systems (1)–(22). Here, the primary emphasis is only on the number of individuals in categories I and V in the systems (1)–(22). Our objective is to use the number of individuals in categories I and V to make predictions specifically for the number of individuals in category I while considering a range of different values for the number of individuals in category V. The LSTM model is configured with a total of 100 hidden layers. The model underwent training using the Adam optimizer, employing the mean absolute error (MAE) loss function over a span of 1000 epochs, divided into 72 batches. The root mean squared error (RMSE) for Fig. 4(a) is 1.432, whereas Fig. 4(b) has a slightly higher RMSE of 2.376. This discrepancy may be attributed to the fluctuation in input values seen at each time step of Fig. 4(b). The projected values have the highest degree of similarity with the input data. Hence, by integrating the solutions of the deterministic and stochastic systems (1)–(22) with the benefits of LSTM, demonstrate superior predictive performance for category I with respect to category V in minimum error. Fig. (5) illustrates the influence of migration on the variability of individuals within category I of system (1). In Fig. 5(a), the migration rate of individuals towards the population demonstrates variability while the migration out rate remains constant. In contrast, Fig. 5(b) illustrates the presence of variation in the migration out parameter while maintaining a constant rate for migration toward the population. It has been observed that an increase in rate of migration towards the population correlates with an upward trend in the number of individuals in category I. On the other hand, a higher rate of migration out leads to a reduction in the number of individuals in category I. Therefore, the movement of the population has implications for the control of such infectious diseases. An illustration of the impact of vaccination and population migration limitations on infectious disease is provided in Supplementary

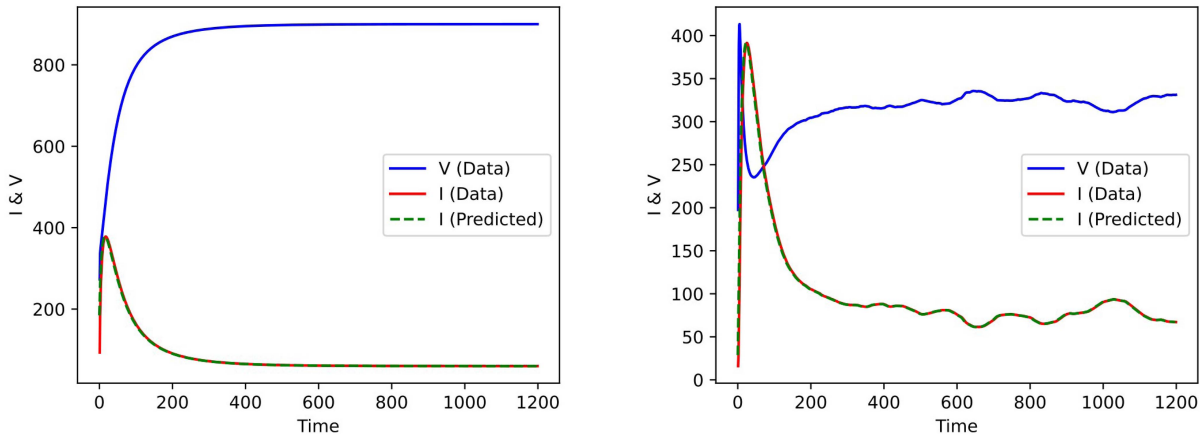

(a) Predicted I with V of system (1)

(b) Predicted I with V of system (22)

Fig. 4. LSTM applied to categories I and V of system (1) and (22).

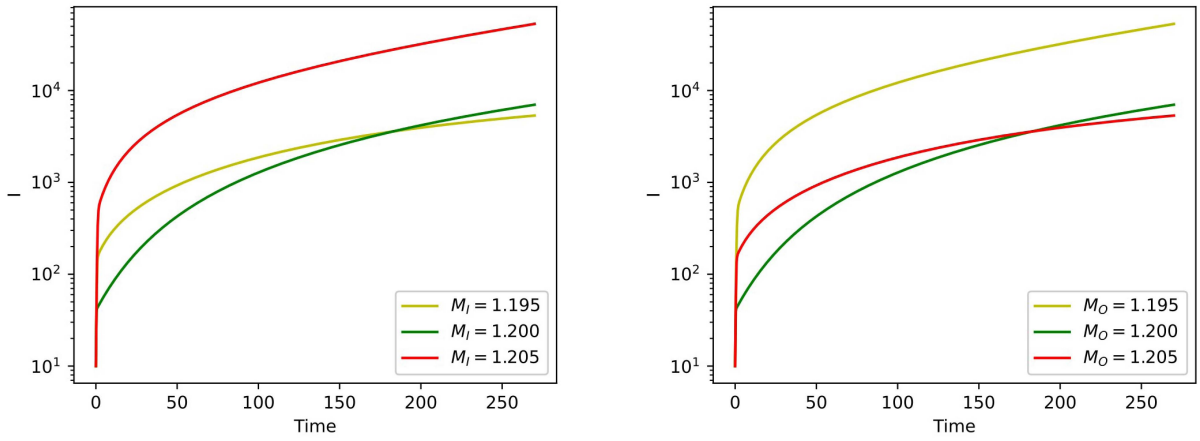

(a) Various M_I with $M_O = 1.2$

(b) Various M_O with $M_I = 1.2$

Fig. 5. Effect of M_I and M_O on category I of system (1) with $\Lambda = 100$, $\delta = 0.05$, $\beta = 0.005$, $\lambda_1 = 0.6$, $\mu = 0.002$, $\gamma_A = 0.001$, $\gamma_I = 0.001$, $\lambda_2 = 0.0006$ and $d = 0.0001$.

Materials VII-G. To investigate the behaviour of the infectious population in the system (27), Fig. (6) is presented, considering the influence of delay parameters. Here, we consider the number of individuals initially in categories S, A, I, and V as 980, 9, 9 and 2, respectively. Interestingly, three distinct patterns are observed for the infectious population in each figure. In Fig. 6(a), the number of individuals in category I exhibits a rapid increase in fluctuations around 50 days, reaching a fluctuation range of -1000 to 1500 cases after 150 days. Notably, these fluctuations occur without a specific periodic pattern. Fig. 6(b) corresponds to a time delay parameter (τ) very close to the one considered in Fig. 6(a). Here, the infectious curve begins to fluctuate at around 45 days and maintains a range between 0 and 1000 cases for approximately 225 days. Subsequently, the fluctuation range expands by 200 cases, both above and below the mean. Fig. 6(c) demonstrates a fluctuation range spanning from -2000 to 2000 cases at 50 days. However, beyond 250 days, the wide range of fluctuations diminishes, indicating that the population has reached the endemic equilibrium. It is worth noting that the fluctuation or bifurcation of the infectious curve does not appear to be solely dependent on the time delay parameter. Instead, it is the periodic values of the time delay parameter (τ) that lead to a higher range of fluctuations, as observed in system (27).

In the analysis of the population dynamics, Fig. 7(a) demonstrates that as the vaccinated population increases, the susceptible population decreases. Higher vaccination rates, coupled with lower vaccination failure rates, result in a rapid transition of the population from the susceptible compartment to the vaccinated compartment, stabilizing at a certain level. The impact of the time delay parameter (τ) is observed as a slight bifurcation in both the susceptible and vaccinated populations before reaching equilibrium. However, the populations of susceptible and vaccinated remain nonzero at equilibrium due to the positive vaccination rate and the possibility of vaccination failure. Moving to Fig. 7(b), higher values of the time delay parameter (τ) are examined, revealing that an increase in the vaccinated population corresponds to a decrease in the susceptible population. With an elevated time delay parameter,

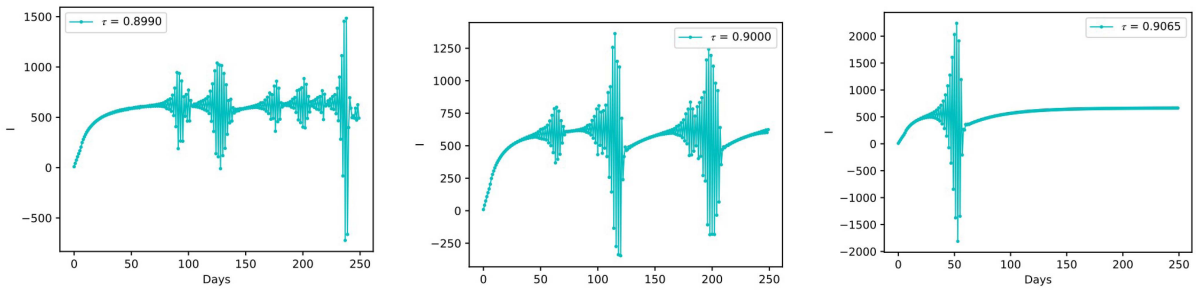

(a) (b) (c)

Fig. 6. Total individuals in category I of the system (27) with $\Lambda = 100$, $M_1 = 0.06$, $M_2 = 0.05$, $\delta = 0.8$, $\beta = 0.02$, $\lambda_1 = 0.8$, $\mu = 0.8$, $\gamma_A = 0.6$, $\gamma_I = 0.7$, $\lambda_2 = 0.1$ and $d = 0.1$.

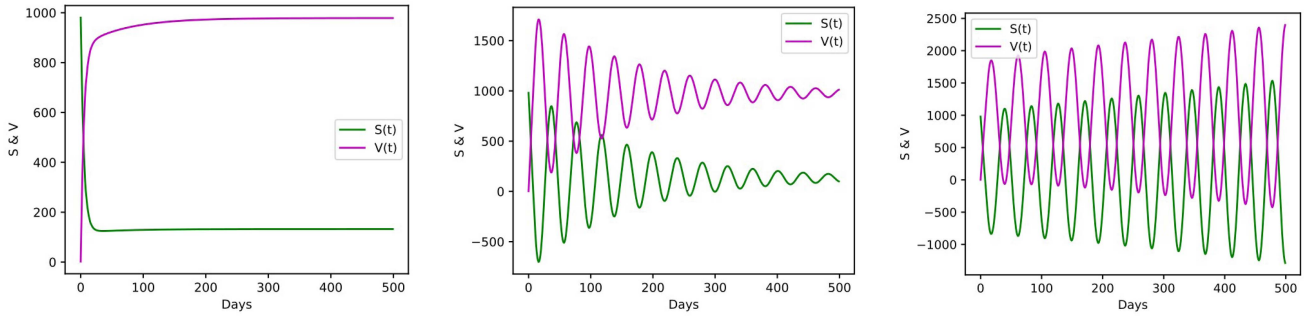

(a) $\tau = 0$ (b) $\tau = 1.676$ (c) $\tau = 1.876$

Fig. 7. Total individuals in categories S and V of the system (31) with $\Lambda = 100$, $M_1 = 0.06$, $M_2 = 0.05$, $\delta = 0.8$, $\beta = 0.02$, $\lambda_1 = 0.8$, $\mu = 0.8$, $\gamma_A = 0.6$, $\gamma_I = 0.7$, $\lambda_2 = 0.1$ and $d = 0.1$.

periodic solutions emerge with a reduced range of fluctuations, eventually converging to equilibrium. Conversely, Fig. 7(c) explores the behaviour of solutions in the system (31) near the critical time delay. As the time delay parameter surpasses the critical value, periodic solutions bifurcate from the equilibrium, exhibiting an increasing amplitude over time with a constant wavelength. These fluctuations signify that the system does not reach equilibrium and becomes unstable. Overall, the analysis highlights the importance of considering vaccination rates, vaccination failure, and the impact of time delay on the population dynamics, revealing stability near equilibrium under specific conditions while indicating instability beyond critical time delays.

VII. Conclusion

In this work, a novel disease modeling by incorporating the migration in the population and vaccination is proposed and the stability of the model is examined by using Lyapunov method and the Volterra integral equation. In addition, a minor perturbation in the infection rate is incorporated into the system to introduce stochasticity and the stability of the system is analyzed by constructing the Lyapunov function. Furthermore, the LSTM model is used to train the solution of deterministic and stochastic systems in order to predict the decline in the number of infectious individuals as the number of vaccinated individuals increases. The delayed system is comprised of two distinct subsystems, one characterized by delay in relation to infection and the other characterized by delay in relation to vaccination. In both systems, it is observable that the endemic equilibrium exhibits unstable due to the occurrence of Hopf bifurcation at certain values of the time delay parameter. The analytical results are shown numerically. Our study provides the influence of a vaccinated population and migrating in and out of the population on the dynamics of a pandemic, contributing to the development of informed strategies and interventions for managing such a pandemic. The assumption of constant parameters may affect the performance of the models. Future research could examine a mathematical model of infectious diseases with parameters that change over time in order to adapt the model to actual data precisely.

Supplementary Materials

In Supplementary Materials, we provide the necessary proofs for all of the lemmas and theorems mentioned in the manuscript. Furthermore, an illustration of an infectious disease affected by vaccination and migratory restrictions in the population is discussed.

Data Availability

The datasets used and analyzed during the current study are available from the corresponding author upon reasonable request.

AUTHORS CONTRIBUTION

Mohammed Salman: Conceptualization, Data curation, Investigation, Validation & Writing original draft. Pradeep Kumar Das: Conceptualization, Investigation, Validation, Writing original draft & Editing. Sanjay Kumar Mohanty: Conceptualization, Data curation, Investigation, Supervision, Validation, Writing original draft & Editing.

CONFLICT OF INTEREST STATEMENT

The authors declare that none of the work reported in this study could have been influenced by any known competing financial interests or personal relationships.

REFERENCES

[1] L. Zhong, L. Mu, J. Li, J. Wang, Z. Yin, and D. Liu, "Early prediction of the 2019 novel coronavirus outbreak in the mainland China based on simple mathematical model," *IEEE Access*, vol. 8, pp. 51761–51769, 2020.

[2] A. AlArjani, M. T. Nasseef, S. M. Kamal, B. S. Rao, M. Mahmud, and M. S. Uddin, "Application of mathematical modeling in prediction of COVID-19 transmission dynamics," *Arabian J. Sci. Eng.*, vol. 47, no. 8, pp. 10163–10186, 2022.

[3] W. O. Kermack and A. G. McKendrick, "A contribution to the mathematical theory of epidemics," *Proc. Roy. Soc. London*, vol. 115, no. 772, pp. 700–721, 1927.

[4] H. A. Adamu, M. Muhammad, A. Jingi, and M. Usman, "Mathematical modelling using improved SIR model with more realistic assumptions," *Int. J. Appl. Sci. Eng.*, vol. 6, no. 1, pp. 64–69, 2019.

[5] T. D. Hollingsworth, "Controlling infectious disease outbreaks: Lessons from mathematical modelling," *J. Public Health Policy*, vol. 30, pp. 328–341, 2009.

[6] O. Diekmann, J. A. P. Heesterbeek, and M. G. Roberts, "The construction of next-generation matrices for compartmental epidemic models," *J. Roy. Soc. Interface*, vol. 7, no. 47, pp. 873–885, 2010.

[7] Y. Enatsu, E. Messina, Y. Nakata, Y. Muroya, E. Russo, and A. Vecchio, "Global dynamics of a delayed SIRS epidemic model with a wide class of nonlinear incidence rates," *J. Appl. Math. Comput.*, vol. 39, no. 1–2, 15–34, 2012.

[8] X. Dai, J. Niu, and Y. Xu, "An efficient numerical algorithm for solving nonlinear Volterra integral equations in the reproducing kernel space," *J. Appl. Math. Comput.*, vol. 69, no. 4, pp. 3131–3149, 2023.

[9] I. W. Suryasa, M. Rodríguez-Gámez, and T. Koldoris, "The COVID-19 pandemic," *Int. J. Health Sci.*, vol. 5, no. 2, pp. 6–9, 2021.

[10] M. Ali, S. T. H. Shah, M. Imran, and A. Khan, "The role of asymptomatic class, quarantine and isolation in the transmission of COVID-19," *J. Biol. Dyn.*, vol. 14, no. 1, pp. 389–408, 2020.

[11] J. F. Oliveira et al., "Mathematical modeling of COVID-19 in 14.8 million individuals in Bahia, Brazil," *Nature Commun.*, vol. 12, no. 1, 2021, Art. no. 333.

[12] M. Suba, R. Shanmugapriya, S. Balamuralitharan, and G. A. Joseph, "Current mathematical models and numerical simulation of SIR model for coronavirus disease-2019 (COVID-19)," *Eur. J. Mol. Clin. Med.*, vol. 7, no. 05, pp. 41–54, 2020.

[13] W. T. Leung et al., "Social contact patterns relevant for infectious disease transmission in Cambodia," *Sci. Rep.*, vol. 13, no. 1, 2023, Art. no. 5542.

[14] N. Tuncer, A. Timsina, M. Nuno, G. Chowell, and M. Martcheva, "Parameter identifiability and optimal control of an SARS-CoV-2 model early in the pandemic," *J. Biol. Dyn.*, vol. 16, no. 1, pp. 412–438, 2022.

[15] J. P. Gutiérrez-Jara, K. Vogt-Geisse, M. Cabrera, F. Córdova-Lepe, and M. T. Muñoz-Quezada, "Effects of human mobility and behavior on disease transmission in a COVID-19 mathematical model," *Sci. Rep.*, vol. 12, no. 1, 2022, Art. no. 10840.

[16] S. P. Brand et al., "The role of vaccination and public awareness in forecasts of Mpox incidence in the United Kingdom," *Nature Commun.*, vol. 14, no. 1, 2023, Art. no. 4100.

[17] M. Martcheva, N. Tuncer, and C. N. Ngonghala, "Effects of social-distancing on infectious disease dynamics: An evolutionary game theory and economic perspective," *J. Biol. Dyn.*, vol. 15, no. 1, pp. 342–366, 2021.

[18] Y. Maki and H. Hirose, "Infectious disease spread analysis using stochastic differential equations for SIR model," in *Proc. IEEE 2013 4th Int. Conf. Intell. Syst., Model. Simul.*, 2013, pp. 152–156.

[19] Y. Cai, Y. Kang, M. Banerjee, and W. Wang, "A stochastic SIRS epidemic model with infectious force under intervention strategies," *J. Differ. Equ.*, vol. 259, no. 12, pp. 7463–7502, 2015.

[20] A. Ríos-Gutiérrez, S. Torres, and V. Arunachalam, "Studies on the basic reproduction number in stochastic epidemic models with random perturbations," *Adv. Difference Equ.*, vol. 2021, no. 1, 2021, Art. no. 288.

[21] J. Yang, Z. Chen, Y. Tan, Z. Liu, and R. A. Cheke, "Threshold dynamics of a stochastic mathematical model for Wolbachia infections," *J. Biol. Dyn.*, vol. 17, no. 1, 2023, Art. no. 2231967.

[22] J. Yu, D. Jiang, and N. Shi, "Global stability of two-group SIR model with random perturbation," *J. Math. Anal. Appl.*, vol. 360, no. 1, pp. 235–244, 2009.

[23] L. F. Gordillo, P. E. Greenwood, and D. Strong, "Epidemic highs and lows: A stochastic diffusion model for active cases," *J. Biol. Dyn.*, vol. 17, no. 1, 2023, Art. no. 2189001.

[24] P. K. Das, S. Meher, R. Panda, and A. Abraham, "An efficient blood-cell segmentation for the detection of hematological disorders," *IEEE Trans. Cybern.*, vol. 52, no. 10, pp. 10615–10626, Oct. 2022.

[25] A. Sahu, P. K. Das, and S. Meher, "High accuracy hybrid CNN classifiers for breast cancer detection using mammogram and ultrasound datasets," *Biomed. Signal Process. Control*, vol. 80, 2023, Art. no. 104292.

[26] P. K. Das, B. Sahoo, and S. Meher, "An efficient detection and classification of acute leukemia using transfer learning and orthogonal softmax layer-based model," *IEEE/ACM Trans. Comput. Biol. Bioinf.*, vol. 20, no. 3, pp. 1817–1828, May/Jun., 2022.

[27] P. K. Das, V. A. Diya, S. Meher, R. Panda, and A. Abraham, "A systematic review on recent advancements in deep and machine learning based detection and classification of acute lymphoblastic leukemia," *IEEE Access*, vol. 10, pp. 81741–81763, 2022.

[28] J. Kim and I. Ahn, "Infectious disease outbreak prediction using media articles with machine learning models," *Sci. Rep.*, vol. 11, no. 1, 2021, Art. no. 4413.

[29] F. Shahid, A. Zameer, and M. Muneeb, "Predictions for COVID-19 with deep learning models of LSTM, GRU and Bi-LSTM," *Chaos, Solitons Fractals*, vol. 140, 2020, Art. no. 110212.

[30] V. K. R. Chimmula and L. Zhang, "Time series forecasting of COVID-19 transmission in Canada using LSTM networks," *Chaos, Solitons Fractals*, vol. 135, 2020, Art. no. 109864.

[31] T. Das and P. K. Srivastava, "Hopf bifurcation and stability switches in an infectious disease model with incubation delay, information, and saturated treatment," *J. Appl. Math. Comput.*, vol. 68, pp. 4135–4159, 2022.

[32] P. Song and Y. Xiao, "Global hopf bifurcation of a delayed equation describing the lag effect of media impact on the spread of infectious disease," *J. Math. Biol.*, vol. 76, pp. 1249–1267, 2018.

[33] B. Shayak and M. M. Sharma, "A new approach to the dynamic modeling of an infectious disease," *Math. Model. Natural Phenomena*, vol. 16, 2021, Art. no. 33.

[34] T. Cheng and X. Zou, "A new perspective on infection forces with demonstration by a DDE infectious disease model," *Math. Biosciences Eng.*, vol. 19, no. 5, pp. 4856–4880, 2022.

[35] M. Salman, S. K. Mohanty, C. Nayak, and S. Kumar, "The role of delay in vaccination rate on COVID-19," *Heliyon*, vol. 9, no. 10, 2023, Art. no. 20688.

[36] P. Van den Driessche, "Reproduction numbers of infectious disease models," *Infect. Dis. Model.*, vol. 2, no. 3, pp. 288–303, 2017.

[37] X. Guan, F. Yang, Y. Cai, and W. Wang, "Global stability of an influenza a model with vaccination," *Appl. Math. Lett.*, vol. 134, 2022, Art. no. 108322.

[38] M. Salman, P. Sahoo, A. Mohapatra, S. K. Mohanty, and L. Rong, "An infectious disease epidemic model with migration and stochastic transmission in deterministic and stochastic environments," *Healthcare Analytics*, vol. 5, 2024, Art. no. 100337.

[39] H. Jelodar, Y. Wang, R. Orji, and S. Huang, "Deep sentiment classification and topic discovery on novel coronavirus or COVID-19 online discussions: NLP using LSTM recurrent neural network approach," *IEEE J. Biomed. Health Informat.*, vol. 24, no. 10, pp. 2733–2742, Oct. 2020.

[40] R. L. Kumar, F. Khan, S. Din, S. S. Band, A. Mosavi, and E. Ibeke, "Recurrent neural network and reinforcement learning model for COVID-19 prediction," *Front. Public Health*, vol. 9, 2021, Art. no. 744100.

[41] S. Tyagi, S. C. Martha, S. Abbas, and A. Debbouche, "Mathematical modeling and analysis for controlling the spread of infectious diseases," *Chaos, Solitons Fractals*, vol. 144, 2021, Art. no. 110707.